Scheme I

1 R = Me; X = Se (37%)
2 R = Et; X = Se (40%)
3 R = Ph; X = Se (12%)
4 R = Me; X = S (45%)
5 R = Et; X = S (50%)

$(MeSi)_4S_6$ (**4**) was synthesized in 45% yield using a procedure similar to that described for (**5**): mp 271-274 °C (lit.[3] 273-276 °C); ^{29}Si NMR ($CDCl_3$) δ 17.0 (lit.[3] δ 16.95).

Results and Discussion

When $RSiCl_3$ (R = Me, Et, Ph) is added to sodium selenide, made in situ from sodium, selenium, and a catalytic amount of naphthalene, the corresponding tricyclo[3.3.1.1^{3,7}]tetrasilaselenane is produced (Scheme I). Likewise if $RSiCl_3$ (R = Me, Et) is added to similarly generated Na_2S, the silicon-sulfur cage systems can be made. All compounds are white, crystalline solids, which decompose over the course of hours if left in air. Decomposition of the selenium-containing molecules produces a reddish solid, presumably including amorphous elemental selenium.

The silicon-sulfur system is well characterized and possesses an adamantane-like structure as determined by X-ray crystal structure analysis.[2] There are two possible structures for a $(RSi)_4Se_6$ cage system given below as A and B. ^{1}H, ^{13}C, and ^{29}Si NMR data will be nearly identical for the two structures except for slight differences in chemical shifts. However, ^{77}Se NMR will discriminate between structures. For A, the ^{77}Se NMR spectra should exhibit one absorption. In B, the ^{77}Se NMR spectra should show two peaks, one signal for the Se atoms in the four-membered rings and another for the Se atoms bridging the two four-membered rings. We observed only one peak in the ^{77}Se spectrum confirming A as the structure.

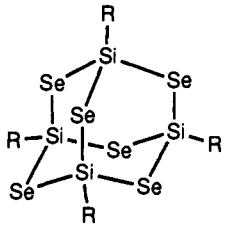

A

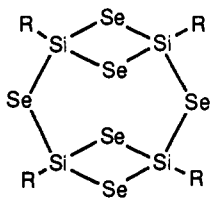

B

Acknowledgment. The financial support of the Air Force Office of Scientific Research through Grant No. 91-0197 and Dow Corning Corp. is gratefully acknowledged.

Contribution from the Department of Chemistry, University of California, Berkeley, California 94720

Synthesis, Structure, and Properties of a Complex That Consists of an $\{Mn_2O_2(O_2CCH_3)\}^{2+}$ Core and a Spanning Hexadentate Ligand

Samudranil Pal, Joel W. Gohdes, Wolf Christian A. Wilisch, and William H. Armstrong*

Received June 27, 1991

Much of the current interest in higher valent polynuclear manganese complexes stems from the fact that such a species is thought to catalyze water oxidation in the photosystem II (PSII) oxygen-evolving complex (OEC).[1] The PSII OEC manganese aggregate has been shown by EXAFS[2] studies to have short (~2.7 Å) Mn···Mn distances[3] and a multiline EPR signal[4] at $g \sim 2$. Binuclear complexes containing the $\{Mn_2O_2\}^{3+}$ core may be thought of as simple models for the water oxidation active site because they possess short Mn···Mn distances and EPR spectra which consist of 16 principal hyperfine lines centered at $g \sim 2$. In the last few years many $\{Mn^{III}Mn^{IV}O_2\}^{3+}$ species have been reported.[5-8] On the other hand, relatively few examples of the $\{Mn^{III}Mn^{IV}O_2(O_2CCH_3)\}^{2+}$ core exist.[9]

One important objective of ours has been to shield one side of an $\{Mn_2O_2\}^{3+}$ core with a hexadentate ligand in order to ensure that the remaining two manganese coordination sites are oriented syn with respect to each other, as shown in I. This structural

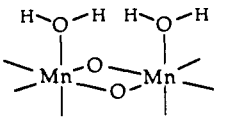

I

type is desirable for at least two reasons: (i) It is possible that the critical step in photosynthetic water oxidation involves O-O bond formation between two terminally ligated O^{2-} or perhaps OH^- groups across the face of an Mn_2O_2 substructure of the active-site manganese complex. Synthetic complexes of the type shown above would allow us to test this hypothesis. (ii) One important structural candidate for the PSII OEC is a dimer of bis(oxo)-bridged dimers.[10] One can easily see that syn-coordinated complexes as depicted above could act as precursors to "dimer-of-dimers" structures. For instance, under basic conditions one might obtain two bis(μ-oxo) dimers bridged together by two

(1) (a) Renger, G.; Wydrzynski, T. *Biol. Met.* **1991**, *4*, 73-80. (b) Debus, R. J. *Biochim. Biophys. Acta*, in press. (c) Dismukes, G. C. *Photochem. Photobiol.* **1986**, *43*, 99-115. (d) Govindjee; Kambara, T.; Coleman, W. *Photochem. Photobiol.* **1985**, *42*, 187-210.

(2) Abbreviations used: PSII, photosystem II; OEC, oxygen-evolving complex; EXAFS, extended X-ray absorption fine structure; EPR, electron paramagnetic resonance; IR, infrared; tppn, *N,N,N',N'*-tetrakis(2-pyridylmethyl)-1,3-propanediamine; tpen, *N,N,N',N'*-tetrakis(2-pyridylmethyl)-1,2-ethanediamine; bpy, 2,2'-bipyridine; phen, 1,10-phenanthroline; tren, $N(CH_2CH_2NH_2)_3$; tacn, 1,4,7-triazacyclononane; cyclam, 1,4,8,11-tetraazacyclotetradecane; DMEPA, ((6-methyl-2-pyridyl)methyl)(2-(2-pyridyl)ethyl)(2-pyridylmethyl)amine; Fc, ferrocene.

(3) Kirby, J. A.; Robertson, A. S.; Smith, J. P.; Thompson, A. C.; Cooper, S. R.; Klein, M. P. *J. Am. Chem. Soc.* **1981**, *103*, 5529-5537.

(4) (a) Hansson, O.; Andreasson, L. E. *Biochim. Biophys. Acta* **1982**, *679*, 261-268. (b) Dismukes, G. C.; Siderer, Y. *Proc. Natl. Acad. Sci. U.S.A.* **1981**, *78*, 274-278.

(5) (a) Brewer, K. J.; Calvin, M.; Lumpkin, R. S.; Otvos, J. W.; Spreer, L. O. *Inorg. Chem.* **1989**, *28*, 4446-4451. (b) Hagen, K. S.; Armstrong, W. H.; Hope, H. *Inorg. Chem.* **1988**, *27*, 967-969. (c) Towle, D. K.; Botsford, C. A.; Hodgson, D. J. *Inorg. Chim. Acta* **1988**, *141*, 167-168. (d) Suzuki, M.; Senda, H.; Kobayashi, Y.; Oshio, O.; Uehara, A. *Chem. Lett.* **1988**, 1763-1766. (e) Collins, M. A.; Hodgson, D. J.; Michelsen, K.; Towle, D. K.; Ludi, A.; Bürgi, H.-B. *Inorg. Chem.* **1986**, *25*, 4743-4750. (f) Plaksin, P. M.; Stoufer, R. C.; Matthew, M.; Palenik, G. J. *J. Am. Chem. Soc.* **1972**, *94*, 2121-2122.

(6) Oki, A. R.; Glerup, J.; Hodgson, D. J. *Inorg. Chem.* **1990**, *29*, 2435-2441.

(7) Goodson, P. A.; Glerup, J.; Hodgson, D. J.; Michelsen, K.; Pedersen, E. *Inorg. Chem.* **1990**, *29*, 503-508.

(8) Cooper, S. R.; Calvin, M. *J. Am. Chem. Soc.* **1977**, *99*, 6623-6630.

(9) (a) Bashkin, J. S.; Schake, A. R.; Vincent, J. B.; Chang, H.-R.; Li, Q.; Huffman, J. C.; Christou, G.; Hendrickson, D. N. *J. Chem. Soc., Chem. Commun.* **1988**, 700-702. (b) Wieghardt, K.; Bossek, U.; Zsolnai, L.; Huttner, G.; Blondin, G.; Girerd, J.-J.; Babonneau, F. *J. Chem. Soc., Chem. Commun.* **1987**, 651-653.

(10) (a) Guiles, R. D.; Zimmermann, J.-L.; McDermott, A. E.; Yachandra, V. K.; Cole, J. L.; Dexheimer, S. L.; Britt, R. D.; Wieghardt, K.; Bossek, U.; Sauer, K.; Klein, M. P. *Biochemistry* **1990**, *29*, 471-485. (b) Guiles, R. D.; Yachandra, V. K.; McDermott, A. E.; DeRose, V. J.; Zimmermann, J.-L.; Sauer, K.; Klein, M. P. In *Current Research in Photosynthesis*; Battscheffsky, M., Ed.; Kluwer Academic Publishers: Dordrecht, The Netherlands, 1990; Vol. 1, pp 789-792. (c) Guiles, R. D. Ph.D. Dissertation, Lawrence Berkeley Laboratory, University of California, Berkeley, CA, 1988. (d) Kuwabara, T.; Miyao, M.; Murata, N.; Murata, T. *Biochim. Biophys. Acta* **1985**, *806*, 283-289. (e) Cheniae, G. M.; Martin, I. F. *Biochim. Biophys. Acta* **1970**, *197*, 219-239.

0020-1669/92/1331-0713$03.00/0

additional oxo or hydroxo bridges. Recently, we have characterized a different sort of dimer-of-dimers structure; one in which a polydentate ligand serves to hold two $\{Mn_2O_2\}^{3+}$ cores together.[11]

With objectives i and ii in mind, we set out to synthesize a "face-capped" $\{Mn_2O_2\}^{3+}$ species using several different hexadentate ligands. We and others have demonstrated[12] that *N,N,N',N'*-tetrakis(2-pyridylmethyl)-1,2-propanediamine (tppn) mediates the assembly of a tetranuclear species that contains two weakly interacting $\{Mn_2O(O_2CCH_3)_2\}^{2+}$ groups. The ethylene analogue of tppn (tpen) seemed somewhat more desirable, as we had shown previously that an $-NCH_2CH_2N-$ moiety spans the $\{Mn_2O_2\}^{3+}$ core in $[Mn_2O_2(tren)_2]^{3+}$.[5b] In this report we demonstrate that, by using tpen, one can indeed prepare the desired face-capped $\{Mn_2O_2\}^{3+}$ core structural type.

Experimental Section

Materials. The ligand *N,N,N',N'*-tetrakis(2-pyridylmethyl)-1,2-ethanediamine (tpen) was prepared by following a reported procedure.[13] The reagent $Mn(O_2CCH_3)_3\cdot 2H_2O$ was purchased from Aldrich Chemical Co. The acetonitrile used in electrochemical experiments was dried by distillation from CaH_2 and stored over 3-Å molecular sieves. The tetraethylammonium perchlorate (TEAP) used as supporting electrolyte was prepared from tetraethylammonium bromide and $HClO_4$ and recrystallized from hot water.[14] All other solvents and chemicals were of analytical grade and were used as received without further purification.

Physical Measurements. IR data were collected on a KBr pellet of $[Mn_2O_2(O_2CCH_3)(tpen)](ClO_4)_2$ (**1**) by using a Nicolet 5DX Fourier transform infrared spectrometer. The electronic spectrum was recorded on a Perkin-Elmer Lambda 9 UV/vis/near-IR spectrophotometer. An IBM 2090D-SRC spectrometer was used to obtain the EPR spectrum. Solid-state magnetic susceptibility measurements were carried out with a Model 800 VTS-50 SQUID magnetometer (SHE Corp.) in the temperature range 5–282 K with an applied magnetic field of 5 kG. A correction for the susceptibility of the empty bucket and a diamagnetic correction (-457×10^{-6} cgsu), calculated from Pascal's constants,[15] were to obtain the molar paramagnetic susceptibilities. Electrochemical measurements were performed with a EG&G PAR Model 264A polarographic analyzer/stripping voltammeter linked with a locally constructed Supercycle triangle wave generator.[16] A platinum-disk working electrode, a platinum-wire auxiliary electrode, and a saturated sodium calomel electrode (SSCE) were used in the three-electrode measurement. The electrochemistry was performed under a dry and purified dinitrogen atmosphere at 298 K. In acetonitrile under conditions identical with those used for **1**, the $E_{1/2}$ of the Fc/Fc^+ couple was 0.39 V (ΔE_p = 80 mV). The potentials reported in this work are uncorrected for junction contributions. Elemental analyses were obtained from the UC Berkeley Microanalytical Laboratory (C, H, N) and Galbraith Laboratories Inc., Knoxville, TN (Mn).

Preparation of $[Mn_2O_2(O_2CCH_3)(tpen)](ClO_4)_2\cdot 3H_2O$ (1). To a solution of 424 mg (1 mmol) of tpen in 15 mL of CH_3OH was added 268 mg (1 mmol) of solid $Mn(O_2CCH_3)_3\cdot 2H_2O$. The mixture was stirred for $^1/_2$ h in the air at room temperature. The resulting brownish green solution was filtered, and to the filtrate was added a CH_3OH solution (5 mL) of $NaClO_4\cdot H_2O$ (140 mg, 1 mmol). A green microcrystalline solid started to precipitate immediately. The mixture was stirred for an additional $^1/_2$ h. The solid was collected by filtration, washed thoroughly with CH_3OH, and dried under vacuum. This procedure afforded 330 mg of **1** (75% yield with respect to Mn). Anal. Calcd for $Mn_2C_{28}H_{37}N_6Cl_2O_{15}$: Mn, 12.51; C, 38.29; H, 4.25; N, 9.57. Found: Mn, 12.79; C, 38.20, H, 4.04; N, 9.52. Significant infrared bands (cm^{-1}): 3420 (br, s), 1608 (s), 1571 (w), 1548 (s), 1485 (s), 1438 (s), 1387 (s), 1340 (s), 1291 (m), 1255 (m), 1094 (vs), 1053 (m), 1031 (m), 930 (m), 771 (s), 697 (sh), 681 (s), 657 (w), 622 (s). Symbols: br, broad; vs, very strong; s, strong; m, medium; w, weak; sh, shoulder.

Table I. Crystallographic Data for $[Mn_2O_2(O_2CCH_3)(tpen)](ClO_4)_2\cdot 2CH_3CN$

chem formula	$Mn_2C_{32}H_{37}N_8Cl_2O_{12}$	V, Å^3	3808.1 (3)
fw	906.48	Z	4
temp, K	183	d_{calcd}, g cm^{-3}	1.581
space group	$P2_1/c$	μ, cm^{-1}	8.466
a, Å	15.027 (2)	λ, Å	0.710 73
b, Å	22.522 (4)	R,[a] %	5.23
c, Å	11.764 (2)	R_w,[b] %	7.89
β, deg	106.965 (16)		

[a] $R = (\sum||F_o| - |F_c||)/\sum|F_o|$. [b] $R_w = \{[\sum w(|F_o| - |F_c|)^2]/\sum wF_o^2\}^{1/2}$; $w = 4F_o^2/[\sigma(I)^2 + (pF_o^2)^2]$, where $p = 0.03$.

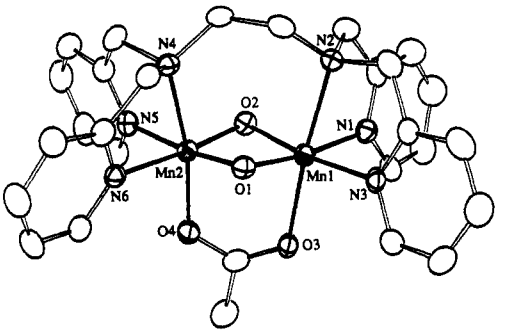

Figure 1. Crystal structure of $[Mn_2O_2(O_2CCH_3)(tpen)]^{2+}$ showing the 50% probability thermal ellipsoids. Hydrogen atoms are omitted, and carbon atoms are unlabeled for clarity.

X-ray Structure Determination. Single crystals of compound **1** were grown by slow evaporation of an acetonitrile–toluene (1:1) solution. A crystal of dimensions 0.5 × 0.5 × 0.6 mm was taken from the mother liquor, immersed in oil (Paratone N, Exxon Chemical Co.), mounted on a glass fiber, and rapidly transferred into a cold stream of nitrogen (183 K). Data were collected on an Enraf-Nonius CAD-4 diffractometer. Unit cell parameters were determined by using 24 reflections, including Friedel pairs, having θ values in the range 12.0–12.3°. Three check reflections were measured every 1 h to monitor the crystal stability. No intensity reduction was observed during data collection. No absorption correction was applied to the data. Crystals of compound **1** have monoclinic symmetry and systematic absences $\{(0k0),\ k = 2n + 1;\ (h0l),\ l = 2n + 1\}$ require the space group to be $P2_1/c$ (No. 14).

The structure was solved by direct methods (SHELXS 86, G. Sheldrick) and refined by standard full-matrix least-squares and Fourier techniques on a Digital Equipment MicroVAX computer using locally modified Enraf-Nonius SDP software.[17] The asymmetric unit contains one molecule of $[Mn_2O_2(O_2CCH_3)(tpen)](ClO_4)_2$ and two CH_3CN molecules. All non-hydrogen atoms except one disordered O atom of one ClO_4^- were refined using anisotropic thermal parameters. Hydrogen atoms of tpen, the acetate methyl group, and one of the CH_3CN molecules were located in a difference map. Hydrogen atom positions were not refined but were included in the structure factor calculations at idealized positions. Significant crystal data are summarized in Table I.

Results and Discussion

Synthesis. Compound **1** is prepared by allowing 1 equiv of $Mn(O_2CCH_3)_3\cdot 2H_2O$ to react with 1 equiv of tpen in methanol in the presence of air. Addition of $NaClO_4$ causes the immediate precipitation of the green complex. If the metal-to-ligand ratio is changed to 2:1, there is no significant increase in the yield. Presently, the mechanism of formation of the $\{Mn_2O_2(O_2CCH_3)\}^{2+}$ core is not well understood. The excess ligand in the reaction mixture reported here is probably acting as a base, which assists in forming the μ-oxo bridges. Elemental analysis fits well for the trihydrate formation $[Mn_2O_2(O_2CCH_3)(tpen)](ClO_4)_2\cdot 3H_2O$. The presence of water of crystallization is also indicated in the IR spectrum.

X-ray Structure. Compound **1** is the third example[9] of the $\{Mn_2O_2(O_2CCH_3)\}^{2+}$ core. The particularly distinguishing feature of **1** is that the hexadentate tpen ligand spans the bis(oxo)-bridged

(11) Chan, M. K.; Armstrong, W. H. *J. Am. Chem. Soc.* **1991**, *113*, 5055–5057.
(12) (a) Toftlund, H.; Markiewicz, A.; Murray, K. S. *Acta Chem. Scand.* **1990**, *44*, 443–446. (b) Chan, M. K.; Armstrong, W. H. To be submitted for publication. (c) Chan, M. K. Ph.D. Dissertation, University of California, Berkeley, 1991.
(13) Mandel, J. B.; Maricondi, C.; Douglas, B. E. *Inorg. Chem.* **1988**, *27*, 2990–2996.
(14) Sawyer, D. T.; Roberts, J. L. *Experimental Electrochemistry for Chemists*; Wiley: New York, 1974; p 212.
(15) Hatfield, W. E. *Theory and Applications of Molecular Paramagnetism*; Boudreaux, E. A., Mulay, L. N., Eds.; Wiley: New York, 1976; pp 491–495.
(16) Woodward, W. S.; Rocklin, R. D.; Murray, R. W. *Chem. Biomed. Environ. Instrum.* **1979**, *9*, 95.
(17) Frenz, B. A. *Structure Determination Package*; B. A. Frenz and Associates and Enraf-Nonius: College Station, TX, and Delft, The Netherlands, 1985; as revised locally by Dr. Frederick J. Hollander.

Table II. Selected Bond Distances and Bond Angles for $[Mn_2O_2(O_2CCH_3)(tpen)](ClO_4)_2 \cdot 2CH_3CN$[a]

	Bond Distances (Å)		
Mn1–O1	1.832 (4)	Mn2–O1	1.790 (4)
Mn1–O2	1.832 (4)	Mn2–O2	1.777 (4)
Mn1–O3	2.196 (4)	Mn2–O4	1.936 (4)
Mn1–N1	2.077 (4)	Mn2–N4	2.057 (4)
Mn1–N2	2.225 (5)	Mn2–N5	2.057 (4)
Mn1–N3	2.068 (4)	Mn2–N6	2.062 (4)
	Bond Angles (deg)		
O1–Mn1–O2	85.65 (16)	O1–Mn1–O3	91.05 (15)
O1–Mn1–N1	172.86 (16)	O1–Mn1–N2	95.49 (16)
O1–Mn1–N3	92.75 (16)	O2–Mn1–O3	90.67 (15)
O2–Mn1–N1	90.39 (16)	O2–Mn1–N2	91.55 (16)
O2–Mn1–N3	171.37 (18)	O3–Mn1–N1	94.93 (16)
O3–Mn1–N2	173.24 (16)	O3–Mn1–N3	97.85 (16)
N1–Mn1–N2	78.67 (18)	N1–Mn1–N3	90.28 (16)
N2–Mn1–N3	80.14 (16)	O1–Mn2–O2	88.58 (16)
O1–Mn2–O4	95.11 (16)	O1–Mn2–N4	90.91 (16)
O1–Mn2–N5	173.61 (18)	O1–Mn2–N6	91.12 (18)
O2–Mn2–O4	94.58 (16)	O2–Mn2–N4	94.49 (18)
O2–Mn2–N5	89.98 (16)	O2–Mn2–N6	174.50 (18)
O4–Mn2–N4	169.23 (18)	O4–Mn2–N5	91.21 (16)
O4–Mn2–N6	90.92 (16)	N4–Mn2–N5	82.99 (18)
N4–Mn2–N6	80.02 (18)	N5–Mn2–N6	89.71 (16)
Mn1–O1–Mn2	91.32 (18)	Mn1–O2–Mn2	91.74 (16)

[a] Numbers in parentheses are estimated standard deviations in the least significant digits.

dimer. The tripodal ends of tpen bind facially to each Mn atom with the aliphatic nitrogen atoms situated trans to the Mn_2O_2 plane. The oxygen atoms of the μ-acetate group and two μ-oxo atoms occupy the other three coordination sites of both Mn atoms (Figure 1). This type of spanning binding mode for tpen has been observed previously in two other cases; the first one was a divanadium(IV) species,[18] and the second, a dichromium(III) complex.[19] As for other compounds containing the $\{Mn_2O_2\}^{3+}$ core,[5a,b,d,f,9a] the Mn(III) and Mn(IV) ions in **1** (Mn1 and Mn2) are clearly distinguishable on the basis of Mn–ligand distances. Selected bond distances and angles are listed in Table II. The Mn1–N2 and Mn1–O3 bonds which are cis to the μ-oxo groups are significantly elongated due to Jahn–Teller distortion. In contrast to the situation for other structurally characterized $Mn^{III}Mn^{IV}$ binuclear compounds,[5-7] the four-membered ring of the $\{Mn_2O_2\}^{3+}$ core in **1** is not planar. This distortion is likely caused by the influence of the bridging acetate group. The dihedral angle between the planes containing Mn1, O1, O2 and Mn2, O1, O2 atoms is 162.7 (1)°. Nonplanar Mn_2O_2 cores were also observed for $[Mn_2O_2Cl_2(O_2CCH_3)(bpy)_2]$ (164.4°)[9a] and $[Mn_2O_2(O_2CCH_3)(tacn)_2](BPh_4)_2$ (160.5°).[9b]

Electronic and Infrared Spectra. The electronic spectrum of compound **1** in acetonitrile (supplementary material) is characteristic of the $\{Mn_2O_2\}^{3+}$ unit.[7] In the cases of the bpy[8] and cyclam[5a] dimers, shoulders at ~800 nm are observed. It has been proposed that this band is due to an intervalence transition.[8] For compound **1** a prominent shoulder is present at 855 nm. There are maxima at 650 (ϵ = 440 M^{-1} cm^{-1}) and 553 nm (ϵ = 360 M^{-1} cm^{-1}). Peaks in this region were observed for other $Mn^{III}Mn^{IV}$ binuclear compounds.[7] Previously it was concluded that oxo to Mn(IV) d_π charge-transfer transitions account for these distinctive bands.[6] On the other hand, similar bands were reported for bpy[8] and cyclam[5a] dimers and assigned to d–d transitions. In addition to the aforementioned peaks, shoulders at 540, 516, 450, and 376 nm are observed for **1**.

A strong peak at 681 cm^{-1} in the infrared spectrum of **1** is believed to be a vibrational mode associated with the Mn_2O_2 core. Similar resonances are observed in the range 679–694 cm^{-1} for the bpy,[8] phen,[8] tren,[5b] and cyclam[5a] complexes and assigned as a vibration of the Mn_2O_2 core. As for the tacn analogue[9b] of **1**, two peaks are observed at 1548 and 1387 cm^{-1}. These are assigned to ν_{as} and ν_s stretches of the μ-acetate group.

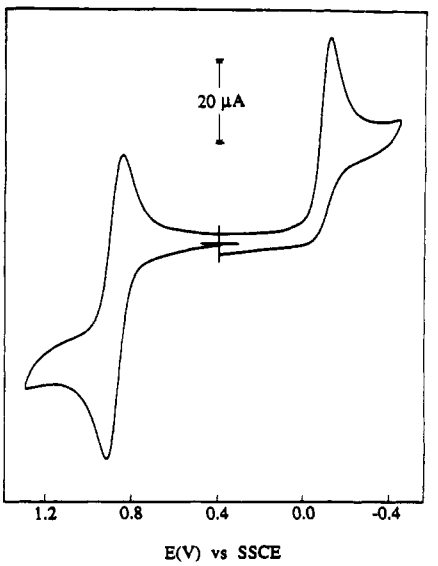

Figure 2. Cyclic voltammogram (scan rate 50 mV s^{-1}) of a 10^{-3} M solution of **1** in acetonitrile (0.1 M TEAP) at a platinum electrode (298 K).

Redox Potentials. The cyclic voltammogram of compound **1** displays a reversible oxidation wave at $E_{1/2}$ = +0.90 V (ΔE_p = 60 mV)[20] and an irreversible reduction at E_{pc} = –0.13 V vs SSCE in acetonitrile solution (Figure 2). The former is assigned to the III,IV/IV,IV couple, and the latter is due to the III,III/III,IV couple. The redox behavior of the other two known compounds containing the $\{Mn_2O_2(O_2CCH_3)\}^{2+}$ unit has not been reported.[9] The IV,IV to III,IV reduction potential is in the middle of the range (0.75–1.26 V) reported[7] for this couple in other binuclear bis(oxo)-bridged dimanganese(III,IV) compounds with predominantly nitrogen terminal donors. The III,IV to III,III wave for **1** is the same as for the $[Mn_2O_2(cyclam)_2]^{3+}$ compound[5a] and has the lowest value in the range observed (–0.13 to +0.29 V) for this type of compound.

Magnetic Susceptibility and EPR Spectrum. A powdered sample of complex **1** was used for variable-temperature magnetic susceptibility measurements in the temperature range 5–282 K. The effective magnetic moment (μ_{eff}) of the dimer decreased gradually from 2.42 μ_B at 282 K to 1.82 μ_B at 119 K. From 119 to 5 K the change in μ_{eff} is relatively small. At 5 K the value of μ_{eff} is 1.71 μ_B, which is in good agreement with the spin-only value predicted for one unpaired electron (1.73 μ_B). These magnetic data were fit (supplementary material) to the expression for χ_M vs T obtained from the isotropic spin exchange Hamiltonian[21] $\mathcal{H} = -2J\hat{S}_1 \cdot \hat{S}_2$, where S_1 = 2 (for the Mn(III) ion) and S_2 = $^3/_2$ (for the Mn(IV) ion). From the best least-squares fit, the values of g and J obtained are 1.982 (1) and –125 (1) cm^{-1}, respectively. The extent of antiferromagnetic interaction between Mn(III) and Mn(IV) ions for **1** is comparable to that of $[Mn_2O_2Cl_2(O_2CCH_3)(bpy)_2]$ (–114 cm^{-1})[9a] but remarkably smaller than that reported for $[Mn_2O_2(O_2CCH_3)(tacn)_2](BPh_4)_2$ (J = –220 cm^{-1}).[9b] Other binuclear complexes with the $\{Mn_2O_2\}^{3+}$ core have J values in the range –146 to –221 cm^{-1}.[6]

The EPR spectrum of complex **1** in frozen acetonitrile–toluene (1:1) solution at 77 K (supplementary material) shows the well-known 16-line pattern centered at $g \sim 2$ with a width of ~1300 G and an average ^{55}Mn hyperfine splitting of 80 G. This spectrum is consistent with the susceptibility data, which indicate predominant population of the S = $^1/_2$ ground state in this temperature range. Among all complexes containing the $\{Mn_2O_2\}^{3+}$

(18) Neves, A.; Wieghardt, K.; Nuber, B.; Weiss, J. *Inorg. Chim. Acta* **1988**, *150*, 183–187.
(19) Toftlund, H.; Simonsen, O.; Pedersen, E. *Acta Chem. Scand.* **1990**, *44*, 676–682.
(20) Meanings of the symbols are as follows: E_{pa}, anodic peak potential; E_{pc}, cathodic peak potential; $E_{1/2} = (E_{pa} + E_{pc})/2$; $\Delta E_p = E_{pa} - E_{pc}$.
(21) O'Connor, C. J. *Prog. Inorg. Chem.* **1982**, *29*, 204–283.

unit, the phen,[22] bpy,[22] tren,[5b] and DMEPA[6] complexes show slight anisotropy in the high-field region. Complex **1** displays evidence of anisotropy in both high-field and low-field regions of the spectrum.

Concluding Remarks. The hexadentate ligand tpen has the appropriate geometry to span across an $\{Mn_2O_2\}^{3+}$ core, thus leaving open two syn-oriented coordination sites that are perpendicular to the Mn_2O_2 plane. The spectral, magnetic, and electrochemical properties of **1** are very similar to those of other species which contain the $\{Mn_2O_2\}^{3+}$ core. In compound **1**, the syn-oriented coordination sites are occupied by a bridging acetate ligand. Our current efforts are directed toward removing this acetate group so that water, hydroxide, and/or other substrate molecules may coordinate to the oxo-bridged dimer.

Acknowledgment. This work was supported by Grant No. GM 382751 from the National Institute of General Medical Sciences.

Supplementary Material Available: For $[Mn_2O_2(O_2CCH_3)(tpen)](ClO_4)_2 \cdot 2CH_3CN$, a fully labeled ORTEP drawing (Figure S1), electronic and EPR spectra (Figures S2 and S3), plots of observed and calculated molar susceptibilities and moments as a function of temperature (Figure S4), and tables of crystal data and data collection parameters (Table S1), atomic positional parameters (Table S2), anisotropic thermal parameters (Table S3), and intramolecular bond distances and angles (Tables S4 and S5) (12 pages); a listing of observed and calculated structure factors (Table S6) (29 pages). Ordering information is given on any current masthead page.

(22) Cooper, S. R.; Dismukes, G. C.; Klein, M. P.; Calvin, M. *J. Am. Chem. Soc.* **1978**, *100*, 7248-7252.

Additions and Corrections

1990, Volume 29

N. Sreehari, Babu Varghese, and P. T. Manoharan*: Crystal and Molecular Structure of Dimeric Bis[*N*,*N*-di-*n*-propyldithiocarbamato]zinc(II) and the Study of Exchange-Coupled Copper(II)-Copper(II) Pairs in Its Lattice.

Pages 4011-4015. The space group of the title compound is $P2_1/c$ rather than $P2_1$. The structure solved in $P2_1/c$ has a final R value of 0.044 and $R_w = 0.047$. Side chains are found to have disorder.

We gratefully acknowledge the suggestions from Dr. Richard E. Marsh of the Beckman Institute at Caltech, Pasadena, CA.

Supplementary Material Available: Tables of fractional coordinates, anisotropic thermal parameters, bond lengths, bond angles, relevant torsion angles, and least-squares mean planes (5 pages); a listing of structure factors (9 pages). Ordering information is given on any current masthead page.—P. T. Manoharan

---

1991, Volume 30

Kimoon Kim,* Won S. Lee, Hee-Joon Kim, Sung-Hee Cho, Gregory S. Girolami,* Philip A. Gorlin, and Kenneth S. Suslick*: Synthesis and Structure of Transition-Metal Bis(porphyrinato) Complexes. Characterization of $Zr(TPP)_2$ and $Zr(OEP)_2$.

Pages 2653-2654. The crystal structure of $Zr(TPP)_2$ was described incorrectly in space group $C2/c$ and should be in the orthorhombic space group *Fddd*. The lattice vectors [100][010][102] define the new *F*-centered cell: $a' = 21.120$ (5) Å, $b' = 21.286$ (6) Å, $c' = 30.805$ (11) Å, $V = 13901$ (7) Å^3, $Z = 8$. The corresponding coordinate transformations are $x' = x - z/2 + 0.25$, $y' = y + 0.25$, and $z' = z/2$. Further refinement with the orthorhombic-averaged data improved the structure, notably the description of the disordered solvate molecule, which is best described as CH_2Cl_2. The new formula of the crystal structure is $ZrN_8C_{88}H_{56} \cdot CH_2Cl_2$ (fw = 1401.63), which is also consistent with the elemental analysis of the bulk material and measured density, as reported. The final residuals were $R_F = 0.058$ and $R_{wF} = 0.060$ for 226 variables and 966 independent reflections with $I > 3\sigma(I)$. This revision did not change the overall structure of the $Zr(TPP)_2$ molecule, which now has exact 222 symmetry, and no changes in bond lengths or angles exceeded previous standard deviations. Revised versions of Tables II and III follow. We thank Dr. R. E. Marsh for bringing this issue to our attention.

Supplementary Material Available: Revised tables of anisotropic thermal parameters, bond distances, bond angles, least-squares planes, and dihedral angles (4 pages); a revised listing of structure factors (5 pages). Ordering information is given on any current masthead page.

Table II′. Positional and Equivalent Isotropic Thermal Parameters for $Zr(TPP)_2 \cdot CH_2Cl_2$[a,b]

atom	x	y	z	B_{eq}, Å^2
Zr	−0.1250	0.3750	0.3750	2.49 (3)
Cl	0.1350 (9)	1.0088 (9)	0.6686 (6)	11.0 (5)*
N1	−0.2152 (3)	0.3454 (3)	0.3332 (2)	2.5 (2)
N2	−0.0938 (3)	0.2846 (3)	0.3337 (2)	2.7 (2)
C1	−0.2662 (3)	0.3825 (4)	0.3227 (3)	2.9 (2)
C2	−0.3163 (4)	0.3453 (4)	0.3049 (3)	3.5 (2)
C3	−0.2960 (4)	0.2859 (4)	0.3027 (3)	3.6 (2)
C4	−0.2336 (4)	0.2855 (4)	0.3198 (3)	3.0 (2)
C5	−0.1958 (4)	0.2318 (4)	0.3199 (3)	2.8 (2)
C6	−0.1309 (4)	0.2321 (3)	0.3261 (3)	2.8 (2)
C7	−0.0921 (4)	0.1782 (4)	0.3202 (3)	3.6 (2)
C8	−0.0317 (4)	0.1972 (4)	0.3223 (3)	3.2 (2)
C9	−0.0323 (4)	0.2638 (4)	0.3293 (3)	2.7 (2)
C10	0.0203 (4)	0.3016 (4)	0.3253 (3)	2.7 (2)
C21	−0.2272 (4)	0.1721 (4)	0.3042 (3)	3.3 (2)
C22	−0.2714 (4)	0.1423 (5)	0.3289 (3)	5.0 (3)
C23	−0.3030 (5)	0.0884 (5)	0.3125 (4)	6.2 (3)
C24	−0.2890 (5)	0.0682 (5)	0.2719 (4)	7.0 (3)
C25	−0.2451 (5)	0.0975 (5)	0.2469 (4)	6.4 (3)
C26	−0.2133 (4)	0.1496 (4)	0.2632 (3)	5.3 (3)
C27	0.0832 (4)	0.2714 (4)	0.3178 (3)	3.2 (2)
C28	0.0941 (4)	0.2320 (4)	0.2824 (3)	4.2 (2)
C29	0.1512 (4)	0.2033 (4)	0.2770 (3)	4.9 (3)
C30	0.2008 (5)	0.2143 (5)	0.3054 (4)	6.2 (3)
C31	0.1902 (5)	0.2554 (5)	0.3401 (3)	5.7 (3)
C32	0.1320 (4)	0.2829 (4)	0.3466 (3)	4.6 (2)
C33	0.125	0.975 (2)	0.625	11 (1)*

[a] The original numbering scheme is retained. [b] Starred values indicate atoms were refined isotropically. Anisotropically refined atoms are given in the form of the isotropic equivalent displacement parameter defined as $(4/3)[a^2B(1,1) + b^2B(2,2) + c^2B(3,3) + ab(\cos\gamma)B(1,2) + ac(\cos\beta)B(1,3) + bc(\cos\alpha)B(2,3)]$.

Table III′. Selected Bond Lengths (Å) and Angles (deg) in $Zr(TPP)_2 \cdot CH_2Cl_2$[a]

Zr-N1	2.390 (6)	Zr-N2	2.400 (6)
N1-Zr-N1′	114.8 (2)	N1-Zr-N1″	73.8 (2)
N1-Zr-N1‴	149.4 (2)	N1-Zr-N2	72.9 (2)
N1-Zr-N2′	74.0 (2)	N1-Zr-N2″	81.6 (2)
N1-Zr-N2‴	135.9 (2)	N2-Zr-N2′	116.0 (2)
N2-Zr-N2″	148.0 (2)	N2-Zr-N2‴	73.3 (2)

[a] Primed atoms are on the same porphyrin pyrrole ring, and double- and triple-primed atoms are on the other ring.

—Kimoon Kim, Gregory S. Girolami, and Kenneth S. Suslick